

Joint Formation of QSOs and Spheroids: QSOs as clocks of star formation in Spheroids

G.L. Granato,^{1,2} L. Silva^{3,2}, P. Monaco⁴, P. Panuzzo², P. Salucci², G. De Zotti^{1,2}, L. Danese²

¹*Osservatorio Astronomico di Padova, Vicolo Osservatorio 5, I35122 Padova, Italy*

²*SISSA, via Beirut 2-4, I34014 Trieste, Italy*

³*Osservatorio Astronomico di Trieste, via Tiepolo 11, I34131 Trieste, Italy*

⁴*Dipartimento di Astronomia, via Tiepolo 11, I34131 Trieste, Italy*

Accepted.... Received.... in original form....

ABSTRACT

Direct and indirect observational evidence leads to the conclusion that high redshift QSOs did shine in the core of early type proto-galaxies during their main episode of star formation. Exploiting this fact, we derive the rate of formation of this kind of stellar systems at high redshift by using the QSO Luminosity Function. The elemental proportions in elliptical galaxies, the descendants of the QSO hosts, suggest that the star formation was more rapid in more massive objects. We show that this is expected to occur in Dark Matter haloes, when the processes of cooling and heating is considered. This is also confirmed by comparing the observed sub-mm counts to those derived by coupling the formation rate and the star formation rate of the spheroidal galaxies with a detailed model for their SED evolution. In this scenario SCUBA galaxies and Lyman Break Galaxies are early type proto-galaxies forming the bulk of their stars before the onset of QSO activity.

Key words: galaxies: formation – dust, extinction – infrared: galaxies – cosmology: theory – quasars: general – dark matter

1 INTRODUCTION

QSOs had been for a long time the main probe of the epoch when galaxies are thought to have formed. Hubble Space Telescope observations, especially the HDF surveys, and ground based observations with the new 10 meter class telescopes, have opened to direct investigation also the early phases of galaxy formation. Exploration of the local Universe is also yielding extremely relevant results to understand the QSO phenomenon. Very high angular resolution photometric and spectroscopic observations have demonstrated that Massive Dark Objects (MDO) are generally present in nearby galaxies endowed with significant spheroidal components (Magorrian et al. 1998; van der Marel 1999). MDOs are thought to be dormant BHs which spent their shining phase as QSOs. Indeed, the MDO mass function well matches the mass function of baryons accreted onto BHs during the QSO activity (Salucci et al. 1999, hereafter paper I). Estimated MDO masses are roughly proportional to those of the spheroidal component of the host galaxy (Magorrian et al. 1998; Gebhardt et al. 2000). This fact implies that high redshift and highly luminous QSOs have been hosted in massive early type galaxies.

In addition, spectroscopic observations of QSO emis-

sion and absorption lines show that high redshift QSOs live in a metal enriched environment (see Hamann & Ferland 1999 for a comprehensive review). Observations at far-IR and sub-mm wavelengths uncovered large amounts of dust in QSOs (Omont et al. 1996; Ivison et al. 1998; Benford et al. 1999; Yun et al. 2000). The dust emission has been ascribed to starburst in the host galaxy (see e.g. Yun et al. 2000; Chapman et al. 1998; Benford et al. 1999) or dust illuminated by the active nucleus (see e.g. Andreani, Franceschini & Granato 1999). The evidence of the dust illuminated by starbursts in high redshift radio galaxies is solid (see e.g. Archibald et al. 2000).

All these pieces of evidence suggest that QSOs at high redshift are active nuclei shining in early type galaxies, during the short fraction of the Hubble time when they were vigorously forming stars and still gas rich. The high metal abundance of the QSO environments strongly supports the idea that the bulk of star formation in host galaxies occurred before the QSO shining phase.

In fact there is evidence that the bulk of stars have formed very soon in elliptical galaxies and in the prominent bulges of the spirals. Cluster elliptical galaxies exhibit a very tight color-magnitude relation, which can be explained if the

arXiv:astro-ph/9911304v2 2 Feb 2001

bulk of their stars formed at very early epochs, corresponding to $z \gtrsim 2$ (Bower et al. 1992; Ellis et al. 1997; Kodama et al. 1998). The very weak dependence of the $M_{g_2} - \sigma$ relation on the galaxy environment suggests that field ellipticals are on average at most 1 Gyr younger than cluster ellipticals (Bernardi et al. 1998). The bulges of spiral galaxies exhibit a tight correlation between the M_{g_2} index and the intrinsic luminosity similar to that of the ellipticals (Jablonka, Martin & Arimoto 1996). These facts support the conclusion that spheroids formed stars very rapidly at early epochs (see e.g. Renzini 1999). The rapid star formation can be strongly reduced or halted by the exhaustion of the gas in most massive objects or by heating and winds, if SN explosions (or the QSO activity itself, as argued below) transfer to ISM even a fraction of their energy (see e.g. Dekel and Silk 1986). For instance galactic winds were brought in the play in order to explain the mass-metallicity relation in elliptical galaxies (Mathews & Baker 1971; Larson 1974). The observed iron abundances in groups and clusters of galaxies can be explained if galactic winds expelled large amounts of enriched gas from spheroids (see e.g. Renzini 1997). Many photometric studies confirm that the massive early type galaxies were practically formed at $z \simeq 1$ with a number density very close to the local one (Im et al. 1996; Franceschini et al. 1998; Schade et al. 1999), even though the issue is still somewhat controversial (e.g. Kauffmann, Charlot & White, 1996; Fontana et al. 1999).

In this paper we present evidence in favour of a strict relationship in the formation of QSOs and their spheroid hosts, with particular emphasis on the timing of star formation in the hosts and the QSO shining. We derive the formation rate of the spheroids from the formation rate of the QSOs (sect 2.1 and 2.2), taking into account the observational and theoretical supports for higher star formation rates (SFRs) in more massive spheroids. In section 3 we present the model (GRASIL) we use to estimate the evolution of the spectral energy distribution (SED) of the spheroids. The model includes dust. In section 4, exploiting the formation rate of spheroids coupled with GRASIL, we argue that the QSO hosts at $z \geq 2$ are the galaxies uncovered in the submillimetre surveys with SCUBA (Blain et al. 1999a,b,c). In section 5 we discuss relationship of the young spheroids with Lyman Break Galaxies (Steidel, Pettini and Hamilton 1995; Steidel et al. 1996; Madau et al. 1996) and in section 6 we investigate the QSO phase. In section 7 we place our results in the context of hierarchical cosmogonies. Section 8 is devoted to a summary.

Unless otherwise specified, the results we present have been obtained adopting a cosmological model with $H_0 = 70 \text{ km s}^{-1} \text{ Mpc}^{-1}$, $\Omega_\Lambda = 0.7$, and $\Omega_M = 0.3$. We also performed the same computations in an Einstein-de Sitter cosmology with $H_0 = 50$. The results, being essentially identical, are not shown. To avoid confusion, we indicate with lowercase t , times measured from the Big Bang, while galactic ages (i.e. times measured from the onset of star formation in a galaxy) are indicated with uppercase T .

2 THE FORMATION OF SPHEROIDAL GALAXIES AS TRACED BY QSO EVOLUTION

The epoch-dependent QSO Luminosity Function (LF) $n_{\text{QSO}}(L_{\text{QSO}}, z)$ is well defined in a large redshift interval $0 \leq z \leq 3$ both in the optical and in the soft X-ray bands (Boyle et al. 1993; Pei 1995; Kennefick et al. 1996; Grazian et al. 2000; Miyaji, Hasinger and Schmidt 2000); also new optical surveys allow sound estimates of the QSO evolution at higher redshift. (Fan et al. 2000). Observations with Chandra X-ray Observatory have shown that most of the Hard X-ray Background (HXR) is due to active nuclei (Mushotzky et al 1999; Giacconi et al 2000; Barger et al 2000). In the following section we will use the Luminosity Function of QSOs, including the 'obscured' ones responsible for a large fraction of the HXR, in order to infer the formation rate of the host spheroidal galaxies.

2.1 The formation rate of spheroids

Since quasar lifetimes Δt_Q are short compared to the typical evolution timescale of their LFs, the rate at which QSOs with BH mass M_\bullet shine at time t_{QSO} (corresponding to redshift z_{QSO}) is related to the LF by:

$$\dot{n}_\bullet(M_\bullet(L_{\text{QSO}}), t_{\text{QSO}}) = \frac{n_{\text{QSO}}(L_{\text{QSO}}, z_{\text{QSO}})}{\Delta t_Q} \frac{dL_{\text{QSO}}}{dM_\bullet} \quad (1)$$

Here n_{QSO} is taken from Pei (1995) for the optical bands, while the contribution from obscured objects is estimated using the LF of Boyle et al. (1993) (see Comastri et al. 1995 and paper I for details). The luminosity of a QSO in a given e.m. band is related to the central BH mass M_\bullet through:

$$L_{\text{QSO}}(M_\bullet) = f_{\text{ED}} L_{\text{ED}}(M_\bullet) / C_B, \quad (2)$$

where C_B is the bolometric correction appropriate for the e.m. band used and $f_{\text{ED}} \equiv L_{\text{bol}} / L_{\text{ED}}$ is the bolometric luminosity in units of the Eddington luminosity. The available data on AGN and QSOs suggest that the ratio f_{ED} is a function of the redshift and/or of the luminosity, going from $\sim 0.05 - 0.1$ for faint local AGNs, to $\gtrsim 1$ for bright high redshift QSOs (see, e.g., Padovani 1989; Sun and Malkan 1989; Wandel 1999). This behaviour can be represented as function of the luminosity by:

$$f_{\text{ED}} = \left(\frac{L_{\text{bol}}}{10^{49} \text{ erg/s}} \right)^{\alpha_{\text{ED}}}, \quad (3)$$

with the exponent α_{ED} set to 0.2 (cfr paper I).

We further assume that quasar lifetimes are proportional to t_{duty} , the e-folding time for the exponential growth of BH mass during QSO activity:

$$\Delta t_Q = K t_{\text{duty}} = K \epsilon \frac{M_\bullet c^2}{L_{\text{ED}} f_{\text{ED}}}. \quad (4)$$

If we adopt $\epsilon = 0.1$ for the mass to radiation conversion efficiency of accretion, we have $t_{\text{duty}} = 4 \times 10^7 \text{ yr}$ for $f_{\text{ED}} = 1$. The value Δt_Q can be inferred by matching the local BH Mass Function with the Mass Function inferred from accretion (Salucci et al 1999), by the QSO clustering properties (Martini and Weinberg 2000) or by matching the space density of high redshift QSOs and the space density of local massive spheroids (Richstone et al 1998; Monaco et al

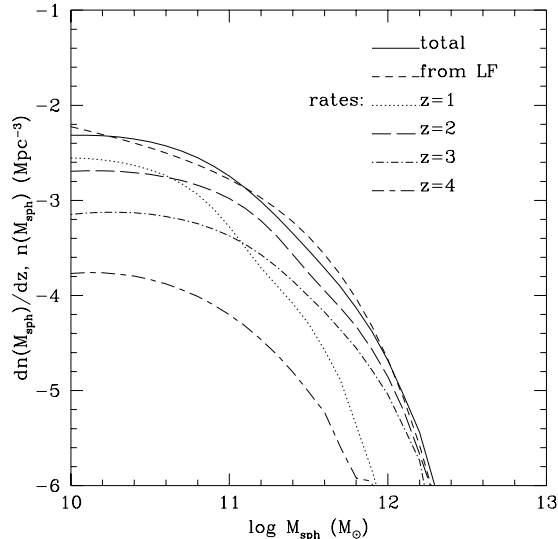


Figure 1. Shining rate of bulges $dn(M_{sph}/dz$ at redshift 1 (dotted thin line), 2 (long-dashed), 3 (dot-dashed) and 4 (short-long dashed). The thick continuous line shows the total mass function of bulges, $n(M_{sph})$, compared to the one inferred in paper I from the local LF of galaxies (thick dashed line).

1999). For instance the analyses of Martini and Weinberg (2000), Salucci et al (1999) and Monaco et al (2000) suggest $\Delta t_Q \sim 8 \times 10^6 - 10^8$ yr.

Using equations (2) and (3) into equation (1) we get:

$$\dot{n}_*(M_\bullet, t_{QSO}) = n_{QSO}(L_{QSO}(M_\bullet), z_{QSO}) \frac{L_{QSO}(M_\bullet)}{M_\bullet} \frac{1}{(1 - \alpha_{ED})} \frac{1}{\Delta t_Q} \quad (5)$$

In order to proceed we introduce here a major assumption, namely that the relationship between the BH mass and the host mass (or velocity dispersion), holding for local spheroids (Magorrian et al 1998; Ferrarese and Merritt 2000; Gebhardt et al 2000), has been imprinted during the early phase of the QSO and host evolution (see e.g. Silk and Rees 1998; Fabian 1999), and has not been changed significantly by subsequent mergers. Then $\dot{n}_*(M_\bullet, t_{QSO})$ is linked to the rate $\dot{n}_{sph}(M_{sph}, t_{QSO})$ at which galaxies endowed with spheroid of present day mass M_{sph} appear to host a QSO at time t_{QSO} by,

$$\dot{n}_*(M_\bullet, t_{QSO}) = \int \dot{n}_{sph}(M_{sph}, t_{QSO}) f(x) dx, \quad (6)$$

where $f(x)$ is the distribution of $x = \log(\frac{M_\bullet}{M_{sph}})$. Data on local objects suggest that $f(x)$ can be represented by a gaussian with mean $\langle x \rangle = -2.6$ and $\sigma = 0.3$ (see paper I). Equating the second members of the two equations above, we get a relationship which, once deconvolved, yield an estimate of $\dot{n}_{sph}(M_{sph}, t_{QSO})$, except for the somewhat uncertain factor $1/(K\varepsilon)$. This residual uncertainty can be eliminated normalizing the result in order to recover the local LF of spheroids. Fig. 1 shows that there is a good agreement between predictions and observations, provided that $K\varepsilon \simeq 0.1$. In the figure the rate $\dot{n}_{sph}(M_{sph}, t_{QSO})$ at different redshift is presented. Integration of $\dot{n}_{sph}(M_{sph}, t_{QSO})$

over time yields their present day mass function. To compare it with data, we use the following relationship between the visible mass of a spheroid M_{sph} and its light:

$$M_{sph}/L = (M/L)_*(L/L_{*E})^{\beta_{sph}-1}, \quad (7)$$

where L_{*E} is the Schechter parameter for the E luminosity function, $\beta_{sph} = 1.25$ and $(M/L)_* = 4.9$ for luminosities in the B band (cfr. paper I). With this recipe the local LF of spheroids is translated into a Mass Function (see e.g. Salucci et al. 1999).

We are mainly interested to high redshift, since we want to test the hypothesis that the QSO activity signals the end of the main episode of star formation in spheroids; in our view the low redshift $z \leq 1$ activity is mostly due to reactivation (see e.g. Kauffman and Haehnelt 2000; Cavaliere and Vittorini 2000). The galaxies associated with QSOs are bright objects. Following the correlation between the bulge luminosity and the BH mass (Magorrian et al 1998) or the correlation between velocity dispersion and BH mass (Ferrarese and Merritt 2000; Gebhardt et al 2000), QSOs, which typically have $L_{bol} \gtrsim 3 \times 10^{45}$ and can be associated to massive BH ($M_{BH} \gtrsim 2 \times 10^7$), are expected to have been hosted in spheroidal galaxies with central velocity dispersion $\sigma \gtrsim 100$ km/s and with present luminosity $M_B \lesssim -18$.

2.2 Early star formation in spheroidal galaxies

In the Introduction we have reviewed several pieces of evidence suggesting that star formation begins in the hosting spheroids at a time t_* and proceeds vigorously at least until the time t_{QSO} , when the QSO shines. Here we estimate the duration of the star formation phase and its possible dependence on the mass.

The statistics on Broad Emission Lines suggest that metallicities are possibly higher in more luminous QSOs (Hamann and Ferland 1993, 1999). This is reminiscent of the mass-metallicity relationship in the local ellipticals and can be naturally explained taking into account the correlation between QSOs and host galaxy luminosities expected on the basis the observed correlation between BH remnants and spheroidal masses.

Large elliptical galaxies exhibit, at least in the central regions, overabundances of magnesium and possibly of other α -elements. Fisher et al (1995) have demonstrated that ellipticals with larger central velocity dispersion σ_0 tend to have larger Mg/Fe . More recently Trager et al (2000b) showed that there is a clear correlation between the ratio E/Fe* within $r = r_e/8$ and the velocity dispersion σ in a significant sample of local ellipticals. Their analysis, extended also to other properties, favours a scenario in which local ellipticals are composed by an old population encompassing $\sim 80\%$ of the stars and by a 20% of 'young' stars. In order to explain the E/Fe- σ correlation and the Z-plane (linking $[Z/H]$, σ and age), two possibilities have been suggested: either the

* "E" refers to the total mass fraction of the elements whose abundance is enhanced in giant elliptical galaxies with respect to Fe; this group is similar but not exactly the same as the α -elements group (for more details see Trager et al 2000a).

IMF flattens with increasing σ , or α elements are more effectively ejected in smaller galaxies due to stronger early winds. The two possibilities are not mutually excluding.

By converse, several authors suggested that in order to reproduce the $[E/Fe]-\sigma$ correlation with reasonable parameters for the IMF and for the SNIa rate and yields, the time scale for the burst must be short ($\sim 0.5-1$ Gyr) for larger masses (see e.g. Matteucci 1994; Thomas, Greggio and Bender 1999).

In the following we will test a scenario in which the star formation begins at t_* and proceeds very rapidly in most massive ellipticals and, at t_{QSO} , the QSO stops the star formation by heating and ionizing the ISM and/or by triggering winds. Afterwards, only minor episodes of star formation can occur, in the sense that they involve $\lesssim 20\%$ of the mass. In order to obtain the observed dependence of E/Fe and Z/H on mass the star formation time scales are shorter (or conversely SFRs are larger) for more massive galaxies.

We adopt for the duration in Gyr of the star formation burst $T_{burst} = t_{QSO} - t_*$ the following parametrization:

$$T_{burst}(M_{sph}) = \begin{cases} T_b^*, & \text{if } M_{sph} \geq M_{sph}^* \\ T_b^* + \log \frac{M_{sph}^*}{M_{sph}}, & \text{if } M_{sph} \leq M_{sph}^* \end{cases} \quad (8)$$

where $T_b^* = 0.5$ Gyr is the burst timescale for galaxies with $M_{sph} \gg M_{sph}^*$ ($M_{sph}^* \simeq 1.5 \times 10^{11} M_\odot$ is the mass of an $L_B^* \simeq 3. \times 10^{10} L_\odot$ elliptical galaxy). In the following we will refer to this parameterization as case A. We also tested a case B, in which star formation lasts $T_{burst} = 0.5$ Gyr for all the spheroids, independently of the mass. It is worth noticing that Monaco et al (2000), in order to account for the observed statistics of QSOs and elliptical galaxies in the framework of hierarchical structure formation, introduced a time delay decreasing with mass between the beginning of the star formation and the QSO bright phase.

It is possible to explore whether the rates of star formation implied by equation 8 are physically plausible in protogalaxies. In a dark halo with circular velocity V_c and mass $M_H \propto V_c^3$, the gas is fed to the star forming regions at a rate which is the minimum between the infall rate and the cooling rate (White and Frenk 1991). The dynamical time is $\tau_{ff}(r) = (3\pi/32G\rho(r))^{1/2}$. The cooling time is defined as the ratio between the specific thermal content of the gas and the cooling rate per unit volume

$$\tau_c(r) = \frac{3}{2} \frac{\rho_g(r)}{\mu m_p} \frac{kT}{n_e(r)^2 \Lambda(T)} \quad (9)$$

where $\Lambda(T)$ is the cooling function, depending also on chemical abundance (Sutherland and Dopita, 1993), and T is the gas temperature. The latter is given by $kT = 1/2 \mu m_p V_c^2$, where μ is the mean molecular weight of the gas and V_c is the circular velocity of the DM halo, whose mass is M_H . Using the relationship between the V_c , the virialization redshift z_{vir} and M_H (White and Frenk 1991) we have

$$T = 35.9 \left(\frac{M_H}{3.3 \times 10^5 M_\odot} \right)^{2/3} (1 + z_{vir}) \text{ K} \quad (10)$$

We use μ appropriate for a fully ionized gas with 25% helium in mass and adopt in the following $z_{vir} = 3$ as a reference value. The total mass of baryons is $M_{tot} = f_b M_H$. We adopted for the baryon fraction $f_b = 0.13$.

In the following we adopt a density profile for the DM appropriate for a Λ CDM cosmology (Navarro, Frenk and White 1997). Depending on mass and density profile, we define a radius r_{cool} inside which the gas can cool and collapse on timescales T_{burst} . We denote by f_{cool} the fraction of baryons within this radius.

In order to explore the SFR, we use the following equation for the evolution of the mass of cool gas $M_{cg}(t)$

$$\dot{M}_{cg}(t) = -(1-R) \frac{M_{cg}(t)}{\tau_*} - \dot{M}_w + C \exp\left(-\frac{t}{\tau_{inf}}\right). \quad (11)$$

The first term on the r.h.s. describes the cool gas converted into stars on a timescale τ_* and the restitution of gas from stars. We assume that $\tau_* = \max(\langle\tau_c\rangle, \langle\tau_{ff}\rangle)$, where the two times are computed using the average density inside r_{cool} , the limiting radius of the star forming gas.

The SFR $= M_{cg}/\tau_*$ is expected to be affected by SN feedback. However the fraction of energy transferred to the gas by the SNaE is rather uncertain. The second term in equation 11 is a plausible description of this feedback (Kauffmann, Guiderdoni and White 1994), and represents the rate of production of 'warm' gas that can not form stars immediately

$$\dot{M}_w(t) = \frac{4}{5} \frac{\nu f_h E_{SN} \text{SFR}}{V_c^2}, \quad (12)$$

where ν is number of SN produced per unit mass of formed stars. We adopt here and in the following a Salpeter initial mass function (IMF), $\Phi \propto M^{-x}$ with $x = 1.35$, between $M_l = 0.15 M_\odot$ and $M_{up} = 120 M_\odot$ and a supernova mass threshold $M_{SN} \geq 8 M_\odot$. With these assumptions $\nu \simeq 8.7 \times 10^{-3} M_\odot^{-1}$. We set the fraction f_h of the SN energy output ($E_{SN} \simeq 10^{51}$ ergs) that is transferred to the gas to 0.15; of course the results for low masses are rather sensitive to the adopted value of f_h .

The last term in equation 11 describes the rate at which cold gas is supplied, namely the 'infall' rate. As for the timescale in the exponential law, we use $\tau_{inf}(r_{cool}) = \max(\tau_c(r_{cool}), \tau_{ff}(r_{cool}))$. The constant $C = M_{tot}/\tau_{inf}$ is the initial rate.

In Fig. 2 the SFR, estimated using equation 11, are presented for spheroids with halo mass $M_H = 1.5 \times 10^{13} M_\odot$ and $M_H = 1 \times 10^{11} M_\odot$. The final masses in stars are $M_{sph} = 4.3 \times 10^{11} M_\odot$ and $M_{sph} = 5 \times 10^9 M_\odot$ respectively. It is apparent that the SFR can be as high as $1000 M_\odot$ in most massive spheroids. In these cases the fraction of the baryons involved in the star forming process is $f_{cool} \simeq 0.2$, since the gas in the outer regions has longer cooling time. At small masses $f_{cool} = 1$, but the effect of SN feedback keeps the SFR low and prolongues the star formation, despite the shorter cooling times.

We exploited equation 11 to compute the SFR for objects with final mass in stars ranging from 10^9 to $5 \times 10^{11} M_\odot$. The SFR, averaged over the time T_{burst} , as function of mass turns out to be

$$\text{SFR} \simeq 100 \left(M_{sph}/1 \times 10^{11} M_\odot \right)^{1.3} M_\odot \text{ yr}^{-1}. \quad (13)$$

Only about 20-40% of the baryons are locked in stars, the rest being in form of warm gas. For large hosts only a small fraction of the gas has a cooling time short enough to collapse before the QSO reionizes, reheats and possibly expels the gas, stopping both star formation and accretion

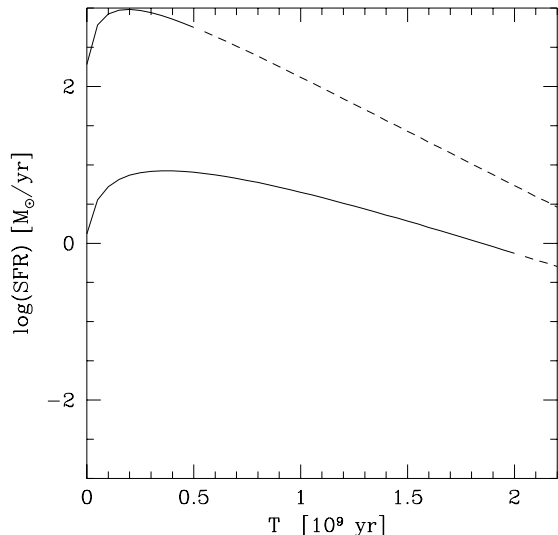


Figure 2. Star Formation Rate for spheroidal galaxies with halo mass $M_H = 1.5 \times 10^{13} M_\odot$ and final mass in stars $M_{sph} = 4.3 \times 10^{11} M_\odot$ (upper curve) and with $M_H = 1 \times 10^{11} M_\odot$ and $M_{sph} = 5 \times 10^9 M_\odot$ (lower curve). The change from solid to dashed line marks the end of the star burst at T_{burst} given by equation 8, because of the QSO shine. In the paper we assume that the SFR vanishes for $T > T_{burst}$.

on the black hole. For small mass hosts, star formation cannot proceed much before the QSO shining because of the efficiency of SN feedback. As a result the stars are again a small fraction about 3-5% of the DM mass.

We checked that the average stellar metallicity increases with the mass. Large SFR in massive hosts rapidly increases the metallicity of the gas and forming stars in such a way that it is about solar before the QSO advent. Conversely in small hosts, the SNe feedback keeps the average SFR low before the QSO blocks the star formation. Thus, although the QSO advent is delayed, nevertheless a lower metal fraction is produced. In our scenario SNIa explode in large hosts after the star formation and QSO output prevent the gas from forming stars. For less massive objects still important episodes of star formation can occur even after the SNIa begins to explode. This produces a positive E/Fe- σ correlation, as observed. The slope of the correlation significantly depends on SNIa progenitors and the ensuing timescale for Fe enrichment (Thomas, Greggio and Bender 1999; Kobayashi, Tsujimoto and Nomoto 1999; Nomoto et al 1999). The details of the chemical evolution will be discussed elsewhere (Romano et al. in preparation).

The rate at which spheroids of present day mass M_{sph} begin to form stars at t_* is directly related to the rate at which they appear to host a QSO (equation 6 and Fig. 1) at time $t_{QSO} = t_* + T_{burst}(M)$.

3 THE SPECTRAL EVOLUTION OF SPHEROIDAL GALAXIES AND THEIR FAR-IR EMISSION

In the previous section we computed the cosmological rate at which spheroids begin their star formation activity. We also estimated how the SFR depend on M_{sph} . To compare with observations we need as well predictions about their SED evolution.

The galaxy surveys at submillimeter wavelengths with SCUBA and analogies with local starburst galaxies suggest that the starburst phase occurred in a dusty environment. The spectrophotometric evolution in the UV and optical bands of bursts of star formation, under the assumption of no or negligible dust absorption, has been investigated by many authors (e.g. Bruzual 1983; Arimoto & Yoshii 1986; Bruzual & Charlot 1993; Bressan, Chiosi & Fagotto 1994). While the no dust approximation well describes the physical situation in elliptical galaxies at later times, dust is expected to play an important role during the starburst epoch. The main effect of dust is to transfer a major fraction of the emitted power from the UV and optical bands to the mid- and far-IR.

In order to compute the SEDs of the spheroids with vigorous star formation and dust, we use the model GRASIL developed by Silva et al. (1998), which is state-of-the-art as far as dust reprocessing is concerned. GRASIL has been tested against UV to radio SEDs of local spirals and starburst galaxies (Silva et al. 1998, Silva 1999). It has also been used to reproduce the IR properties of local galaxies in the framework of semi-analytical models (Granato et al 2000). GRASIL includes: (i) chemical evolution; (ii) dust formation, assumed to follow the chemistry of the gas; (iii) integrated spectra of simple stellar populations (SSP) with the appropriate chemical composition; and (iv) appropriate distribution of stars, molecular clouds (in which stars form and subsequently escape) and diffuse dust. In particular, dust is spread over the whole galaxy and its temperature distribution is determined by the local radiation field. It is noteworthy that the assumption of a single dust temperature turns out to be a significant oversimplification.

The predictions of sub-mm fluxes are plagued by the uncertainty of the far-IR wavelength dependence of the dust emissivity which, *convolved with the temperature distribution of dust grains*, determines the sub-mm steep slope of the SED. Longward of $\sim 40\mu\text{m}$ the dust opacity can be represented by a power law $k_\nu \propto \nu^\gamma$. Values ranging between 1 and 2 are commonly adopted for the spectral index γ . The classical computations by Draine and Lee (1984) predict $\gamma = 2$, but there are several indications of a shallower slope at least in some cases. The issue is further confused by the fact that in most papers the observed sub-mm continuum is fitted with single temperature gray bodies. However, Silva et al. (1998) found that the IR spectrum of the archetypal ultraluminous infrared galaxy (ULIRG) Arp 220 is well represented by $k_\nu \propto \nu^{1.5}$, whilst $k_\nu \propto \nu^2$ is more suitable for M82, the prototype starburst galaxy, and other galaxies. Arp 220 may however be more representative of a spheroid. Since a single opacity law may be too strong an assumption we treat γ as a free parameter allowed to vary between 1 and 2.

In Figs. 3 and 4 model SEDs for elliptical galaxies

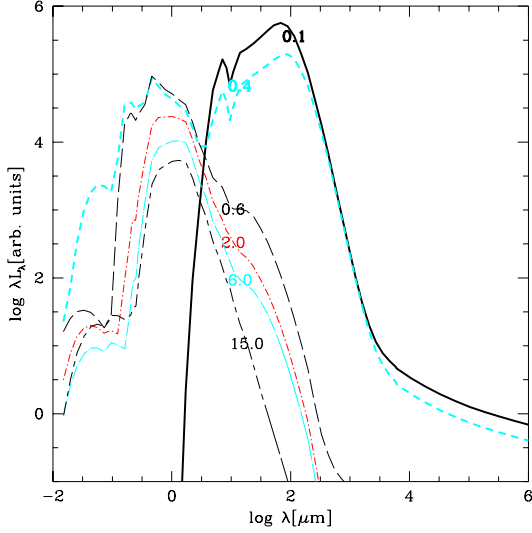


Figure 3. Model SEDs of elliptical galaxies before (thicker lines) and after (thinner lines) the QSO activity for $T_{burst} = 0.5$ Gyr. Numbers along the curves are the age in Gyr of the corresponding models.

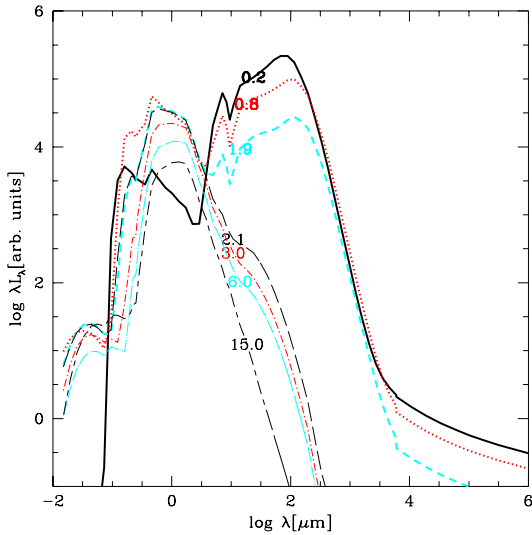


Figure 4. Same as the previous figure but for $T_{burst} = 2$ Gyr

are shown as a function of time adopting $\gamma = 1.5$. In the former case, gas and dust are removed and star formation is stopped at $T_{burst} = 0.5$ Gyr (corresponding to the SFR in the upper curve of Fig. 2), while in Fig. 4 $T_{burst} = 2$ Gyr (lower curve of Fig. 2). It is worth noticing that GRASIL predicts that the fraction of bolometric luminosity emitted in the far-IR decreases with time during the burst phase. In the case depicted in Fig. 4 this fraction declines from about 90% to about 40%.

At the end of the burst, gas and dust are removed and the stars already formed emerge and shine in the optical bands, while the far-IR luminosity drops dramatically. Of course both cases exhibit the same behavior at $T \gg T_{burst}$. However, the model with $T_{burst} = 0.5$ Gyr passes through

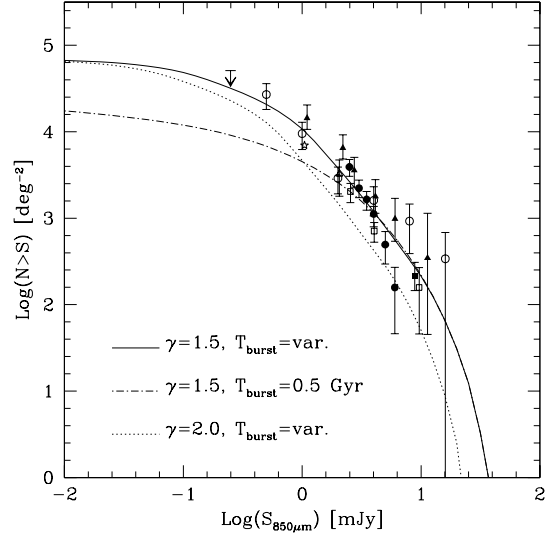


Figure 5. Predicted contributions of the spheroids to $850 \mu\text{m}$ counts. Solid line is for case A (T_{burst} given by equation 8) and $k_\nu \propto \nu^{1.5}$ while dot-dashed line is for case B ($T_{burst} = 0.5$ Gyr and $k_\nu \propto \nu^{1.5}$). Data are from Blain et al. (1999b) (open circles), Hughes et al. (1998) (star and open triangles), Barger, Cowie and Sanders (1999) (open squares) Eales et al. (2000) (filled circles), Chapman et al. (2000) (filled triangle) Borys et al. (2000) (filled squares).

a relatively blue phase (in the rest frame) during the first Gyr after the onset of the galactic wind, while in the case $T_{burst} = 2$ Gyr, the galaxy emerges with redder colours.

The UV and optical luminosities of the spheroids during the starburst dusty phase critically depend on the relative distribution of stars and dust, which sets the small fraction of UV luminosity escaping from molecular clouds (where stars are born). Therefore any model has large uncertainties, and only observations can enlighten the physical processes involved. For instance, local starburst galaxies, which are both strong IR emitters and relatively blue objects, are well reproduced by GRASIL, allowing stars to emerge from rather thick clouds ($\tau(1\mu\text{m}) \sim 30$, as typical in the Galaxy) on timescales of the order of 10^7 yr (Silva et al. 1998). Conversely Silva (1999) has shown that a very red optical spectrum, resembling that of the Extremely Red Object HR 10 (Hu & Ridgway 1994; Cimatti et al. 1998; Dey et al. 1999), can be obtained assuming longer timescales for the escape of stars from molecular clouds, endowed with much lower optical thickness ($\tau(1\mu\text{m}) \sim 2$). On the other hand the SED predictions are more robust in the far-IR, the most important uncertainty being related to the dust opacity spectral index γ discussed above.

The radio emission is computed starting from the type II SN rate (Condon & Yin 1990), under the assumption that all stars with mass $M_{SN} \geq 5 M_\odot$ end in a SN; the radio luminosity has to be decreased by a factor ~ 2 if $M_{SN} \geq 8 M_\odot$ is assumed (see Silva 1999 for details).

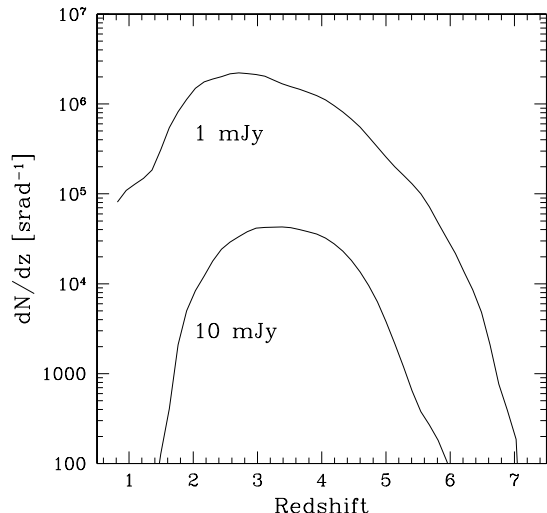


Figure 6. Predicted redshift distribution of spheroids brighter than 1 mJy and 10 mJy at 850 μm for case A.

4 THE SUBMILLIMETER COUNTS AND THE DURATION OF THE BURST IN SPHEROIDS

In our scheme we identify the observed galaxies with $S_{850} \gtrsim 1$ mJy with the dusty starbursts, occurring in spheroidal galaxies before the shining of the QSO. From Figs. 3 and 4 it is apparent that the duration T_{burst} of the dusty starburst can be tested by far-IR counts and related statistics.

Coupling the SED predicted by GRASIL with the formation rate of the spheroids $\dot{n}_*(M_{sph}, t_*)$, we compute the expected contribution of spheroids to the submillimeter galaxy counts. The parameters mainly affecting the fit to observed counts are the spectral index of dust emissivity γ and T_{burst} .

With the assumption $T_{burst} = 0.5$ for all masses, the spheroids would reproduce 850 μm counts only at brightest fluxes, allowing for a substantial contribution from an additional population of possibly lower redshift objects. By converse with a burst duration depending on the mass as in case A (equation 8) we obtain an excellent fit to the observed counts with $\gamma = 1.5$, as shown in Fig. 5. Therefore in the following we concentrate on this solution, unless otherwise explicitly stated.

It is worth noticing that also a longer duration of the burst $T_{burst} = 2$ Gyr, with a corresponding decrease in SFRs, could give an acceptable fit to the counts, provided that $\gamma = 2$ is adopted. However this solution is not satisfactory, since it would decrease the the Mg/Fe ratio below the average observed value for local elliptical galaxies $Mg/Fe \simeq 0.2$ (Kobayashi and Arimoto 1999; Trager et al. 2000 a,b).

Since in our scheme the infrared emission in the spheroids occurs before the QSO shine, the SCUBA sources must be located at high redshift. For fluxes $S_{850} \gtrsim 1$ mJy, the predicted redshift distribution is relatively broad, with almost all the sources lying in the redshift interval $2 \lesssim z \lesssim 5$ (Fig. 6). However we predict a non negligible number of

sources at $z \gtrsim 5$. Even at a flux limit $S_{850} \gtrsim 10$ mJy almost all the sources are predicted to lie at $z \gtrsim 2$. This is in agreement with the results obtained so far by the spectroscopy of the optically identified counterparts of SCUBA sources (Blain et al. 1999c; Smail et al. 2000). A testable prediction of the proposed scheme is that there are more extragalactic sources with $S_{850} \gtrsim 1$ mJy at $z \geq 5$ than at $z \leq 1$, where only $\lesssim 1\%$ are located.

The model source counts at $S_{850} \gtrsim 1$ mJy are dominated by the massive spheroids (E/S0 galaxies), which have presently large luminosities $M_B \leq M_{B*} \simeq -20.5$.

How do the properties of the starbursting spheroids compare with those of the individual submillimeter galaxies? The estimates of SFR for SCUBA galaxies range from several hundreds to a few thousands $M_\odot \text{yr}^{-1}$ (Iverson et al 2000; Frayer et al 2000) Two SCUBA sources have been optically identified with Extremely Red Objects. The available optical identifications point toward very faint ($I \geq 26 - 27$) counterparts (Smail et al. 1999). In our model, the most massive spheroids have SFR ranging from several hundred to thousand $M_\odot \text{yr}^{-1}$ and they are faint at UV and optical wavelengths during the dusty phase. However, it is worth mentioning that the expected optical magnitudes and colours of these high z objects are very sensitive to the tiny fraction of UV emission surviving after dust extinction and can in practice span a large range of values, even at a fixed redshift. For instance, we can reproduce the 850 μm source counts with objects exhibiting, during the dusty phase, colours similar to those of EROs, as well as with relatively bluer ones. This can be achieved simply by tuning the small fraction of young stars which have already moved out from the parent clouds and/or on the typical optical depth of clouds (cfr. sect. 3 and 5).

The extraordinary bursts of star formation before t_{QSO} result also in large radio luminosities. Our scenario predicts that the 850 μm sources with $1 \lesssim S_{850} \lesssim 10$ mJy have radio fluxes at 5 GHz in the range $5 \lesssim S_5 \lesssim 200$ μJy , in agreement with the first results on the radio emission of SCUBA galaxies obtained by Smail et al. (2000) and with the findings of Barger, Cowie and Richards (2000).

At 450 μm Blain et al. (1999c) report $N(> S = 10 \text{ mJy}) = 2.1 \pm 1.2 \times 10^3 \text{ deg}^{-2}$. We predict that at this flux level the dusty spheroids are $0.7 \times 10^3 \text{ deg}^{-2}$, a significant fraction of the counts. By contrast, at 175 μm the expected contribution is negligible at the bright limit $S_{175} \sim 100$ mJy (Puget et al. 1999; Kawara et al. 1998). This is due to the fact that the K-correction is not as favourable as it is at longer wavelengths, dimming sources at $z \gtrsim 3$, where most of the dusty spheroids are located (cfr. Fig. 6). Indeed Scott et al. (2000) have observed with SCUBA at 450 and 850 μm a subsample of the objects selected at 175 μm . The resulting submillimeter spectral energy distributions suggests that these objects are at low or moderate redshift $0 \leq z \leq 1.5$.

Going to shorter wavelengths, the spheroids emerge as an important component below 10 mJy at 60 μm ; at 90 μm , they start to be a non negligible fraction at fluxes $\lesssim 20$ mJy. The latter limit is within the reach of the ELAIS survey, covering about 20 square degrees at 90 μm (Efstathiou et al. 2000).

Several authors presented models of galaxy evolution

tailored to fit available data and in particular the submillimeter counts. For instance Guiderdoni et al (1998) reproduced the counts by imposing a large evolution in the fraction of mass density involved in bursts of star formation and in the fraction of Ultra Luminous Infrared Galaxies (ULIGs), both fractions passing from a few percent in the local Universe to substantial values at high redshift. The conclusion that rapid star formation activity is required at $z \gtrsim 3$ has been claimed by Blain et al. (1999a). They showed that, in order to reproduce the observed sub-mm counts, the activity in galaxies had to be a factor of 200 larger at $z \sim 3$ than in the local Universe. In their scheme this activity refers to both starbursts and to AGNs, and is triggered by merger events at high redshift in a hierarchical model of galaxy formation. A view even closer to our own has been proposed by Tan, Silk & Balland (1999). They exploited a model in which the final morphology of the galaxies depends on the number of collisions and tidal interactions they suffer (Balland, Silk & Schaeffer 1998), deriving for spheroids large star formation rate density at high redshift. In particular, they broadly reproduce the $850 \mu\text{m}$ counts with objects that suffered important collisions and that they identify as precursors of spheroidal objects.

Our model is characterized by a very steep increase of the counts below $\simeq 60 \text{ mJy}$. Above this flux limit the sources are mainly low redshift spirals and starburst galaxies, while just below it a large amount of high redshift star forming spheroids appear.

In conclusion the most massive spheroids bursting at $z \gtrsim 2$, before the onset of the QSO activity, can be identified with the observed SCUBA sources down to 1 mJy . The SCUBA galaxies are strongly clustered, since they are shining in the most massive virialized haloes at high redshift. The large rate at which the spheroids form at high redshift, is dictated by the QSO luminosity function and by the short QSO lifetime Δt_Q . The other relevant parameter is the duration of the star formation, observationally bounded also by the chemical evolution of QSO hosts and in general of elliptical galaxies. The implied star formation rates are physically plausible in protogalaxies (cfr Sect. 2.2).

5 STARBURSTING AND POST-STARBURST SPHEROIDS AND LYMAN BREAK GALAXIES

In the context of the star formation in spheroids at high redshift, a relevant issue is the relation of high redshift galaxies selected in optical and near IR bands with the submillimeter selected galaxies. Steidel et al. (1999), using a galaxy sample complete to $I_{AB} \lesssim 25$ and appropriate color criteria, were able to identify a large sample of galaxies with the Lyman Break falling in the optical or near UV bands. These objects at $z \geq 3$ have been claimed to exhibit dust absorption with reddening in the range $0 \leq E(B - V) \leq 0.4$, with an average value of ~ 0.15 (Steidel et al. 1999). After correction for the implied dust extinction, the UV luminosity density of the LBGs at $z \sim 3 - 4$ would be almost equal to that inferred from galaxies lying at $z \sim 1$ (Connolly et al. 1997). The corresponding extinction corrected (by a factor of about 5) star formation rate of a typical M_* galaxy would

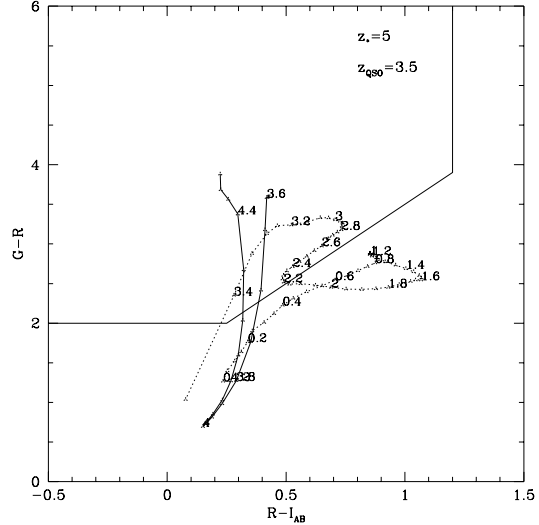


Figure 7. Track of the model of Fig. 1, assumed to begin star formation at $z_* = 5$, in the two colour plane ($G - R$) vs. ($R - I$) used by Steidel et al. (1999) to select LBG candidates. The upper left region bounded by solid lines is the selection region. Number along the track (solid line before the wind and dotted afterwards) are the corresponding redshifts.

be of about $60 M_\odot \text{ yr}^{-1}$. This implies a SFR per unit volume almost constant $\dot{\rho}_{SFR} \simeq 0.15 M_\odot \text{ yr}^{-1} \text{ Mpc}^{-3}$ from $z \sim 1$ to $z \sim 4$.

On the other hand SCUBA observations of a selected subsample of LBGs resulted in only one possible detection, suggesting that the SFR of the population as a whole is possibly low (Chapman et al. 1999). However this result is expected in our scheme, because of selection effects (see also Adelberger and Steidel 2000; Peacock et al. 2000). The UV luminosity during a star burst critically depends on the fraction of young stars already escaped from their parent molecular clouds and on the associate time scale (cfr. Section 3 and Silva et al. 1998). We already remarked that it is more prone to model uncertainties than the IR and sub-mm emission. In any case, the typical behavior of our models is shown in Fig. 1 and Fig. 2. The ratio L_{FIR}/L_{UV} varies from 5-10 at about the end of the burst to very large values just after the begin. After the QSO phase the ratio falls down very rapidly, in the short period when the spheroids are still blue unextincted objects.

Keeping in mind the above mentioned caveats concerning the dusty star-forming phase, our modelling predicts that the spheroids may spend most of their $z \geq 3$ life inside the region of the colours plane used to select the LBG candidates (Steidel et al 1999). For instance, a massive galaxy $M_{sph} \simeq 3 \times 10^{11} M_\odot$ with star formation started at $z_* \simeq 5$ and with the QSO activity appearing after $T_{burst} \simeq 0.5 \text{ Gyr}$, would have $I_{AB} \lesssim 25$ since $z \lesssim 4$, and would exhibit colours ($G - R$) and ($R - I$) quite similar to those of the LBGs, as evidenced by Fig. 7.

In our scenario the hosts of bright QSOs ($L_{bol} \geq 10^{13} L_\odot$) may appear as LBGs both during their starburst phase and soon after the QSO shining; these hosts now have luminosities $M_B \lesssim -20.5$ and velocity dispersion $\sigma \simeq 200$

km/s. As stated in section 4, these hosts are also seen as SCUBA objects during their starburst, since they have average a SFR in the range $100\text{--}1000 M_{\odot} \text{ yr}^{-1}$. The metal abundance of their stars, estimated with a Salpeter IMF, is about solar. These massive spheroids are also expected to exhibit a large rate of SNIa explosion, after the QSO shining, when they are almost gas and dust free.

Less massive spheroids, with present luminosities $-17 \leq M_B \leq -20.5$, at redshift $z \sim 3$ have average SFR from a few to one hundred $M_{\odot} \text{ yr}^{-1}$ and sub-solar metal abundance in stars, decreasing with decreasing SFR. The majority of these spheroids have not yet experienced the QSO shining at $z \geq 3$ and they are in the pre-QSO phase. In our modelling of the SED (cfr. sect 3) dust follows the gas chemistry and, as a consequence, the extinction is expected to decrease with decreasing SFR. Thus the less massive spheroids can appear as LBGs and may constitute a major fraction of them. In conclusion the spheroids independently of their mass very likely showed up at $z \geq 3$ as LBGs. However they have SFR, metal abundance, dust extinction and clustering scale decreasing with their mass.

It is also worth noticing that in our schematic model star formation has completely stopped after t_{QSO} . However, ionization, heating and winds due to the QSO can simply decrease the SFR from several hundred $M_{\odot} \text{ yr}^{-1}$ to several $M_{\odot} \text{ yr}^{-1}$, compatible with the observed UV emission from a typical LBG. Since this more prolonged star formation would involve only a minor fraction of the galaxy mass, say 5-10 per cent of the mass in 1-2 Gyr, the present day spectra of the galaxy would be unaffected. A residual low level of star formation activity has been inferred from broad band spectra of the HDF elliptical galaxies at $z \sim 1$ (Franceschini et al. 1998).

6 THE QSO PHASE

The QSO can heat, ionize and also expel the ISM, thus strongly decreasing or even stopping the copious star formation in the host galaxy at t_{QSO} (Silk and Rees 1998; Fabian 1999). However still significant star formation can be present during the QSO lifetime $\Delta t_Q \sim 4 \times 10^7$ yr. Several objects with these characteristics have already been found (e.g. Omont et al. 1996; Ivison et al. 1998; Benford et al. 1999; Yun et al. 1999). If we assume that the star formation is not quenched during the nuclear activity, then the fraction of QSOs in an unbiased submillimeter survey depends on the ratio between the QSO lifetime and the burst duration T_{burst} . Since the latter timescale in our scheme is a function of the mass, this precise fraction depends on the flux limit. In particular for bright submillimeter sources $S_{850} \gtrsim 2$ mJy we expect $T_{burst} \simeq 0.5\text{--}1$ Gyr and then a fraction of QSOs from a few to 10% is estimated. Recent observations of SCUBA galaxies with Chandra suggest that they are mainly powered by starbursts, unless Compton-thick tori with little circumnuclear X-ray scattering are in place (Fabian et al 2000; Hornschemeier et al 2000; Severgnini et al 2000). A rather different result has been obtained by Bautz et al (2000), who were able to detect the X-ray counterparts of two submillimeter sources in A 370. These authors conclude that $20^{+30}_{-16}\%$ of the submillimeter galaxies exhibit X-ray emission from AGN. Spectroscopy revealed no QSO among the

15 850 μm selected sources, though several of them exhibit possible signs of low nuclear activity (Ivison et al. 2000).

On the other hand hard X-ray selected sources down to $S_{2-10\text{keV}} \sim 2\text{--}4 \times 10^{-15}$ ergs $\text{s}^{-1} \text{ cm}^{-2}$ are basically not detected even in deep submillimeter exposures $S_{850} \gtrsim 2$ mJy (Barger et al 2000; Fabian et al 2000; Severgnini et al 2000), with a few exceptions. In particular in the sample of Barger et al (2000) most of the X-ray contribution to the resolved X-ray background comes from AGN with $L_{bol} \sim 10^{45}\text{--}10^{46}$ erg s^{-1} , associated to BH masses $M_{BH} \sim 10^7\text{--}10^8 M_{\odot}$ and baryon masses in spheroids $M_{sph} \sim 5 \times 10^9\text{--}5 \times 10^{10} M_{\odot}$, in keeping with the predictions of Salucci et al (1999). At 850 μm , contributions from dusty tori around the active nucleus and from star bursts in host galaxies are expected. However the dust emission from the torus peaks at $\lambda \simeq 30 \mu\text{m}$, though in case of very extended structures a wide spread of temperatures tends to produce a plateau up to 80 μm (Granato and Danese 1994; Efstathiou & Rowan-Robinson 1995). Thus relatively faint AGN at $z \sim 1\text{--}2$ can not be detected at $S_{850} \geq 1$ mJy. Also the starburst emission is elusive, because of the relatively low star formation expected in these objects. For instance in our model we expect that their host galaxies have already formed most of their stars in about 1-2 Gyr, with an average $SFR \sim 2.5\text{--}50 M_{\odot} \text{ yr}^{-1}$. These limits are below possible detection by SCUBA for galaxies at $z \geq 1$. Then, as claimed by Granato, Danese & Franceschini (1997), the obscured AGNs, which produce a major fraction of the Hard X-ray Background Radiation (HXRb), contribute only a small fraction of the FIRB at submillimeter wavelengths (see also Gunn and Shanks 1999).

Interestingly enough, the evolutionary links between the star bursting phase and the nuclear activity we have envisaged at high redshift, can be applied to ultra luminous infrared galaxies at low redshift (Sanders et al. 1988). In our scheme the low redshift ULIRGs correspond to the dusty starburst phase. This is in keeping with recent ISO observations that show that for the local ULIRGs, the starburst activity is sufficient to power the bulk of the bolometric luminosity (Genzel et al. 1998). However we also expect cases in which the QSO light reprocessed by dust in the host galaxy is dominating over the far-IR emission due to the starburst.

7 DISCUSSION

7.1 QSO hosts

A major assumption in our model is that the relationship between BH mass and host galaxy mass has been imprinted at early epochs (section 2.1). Recent observations from ground and with HST show evidence that the radio loud QSO and the radio galaxies at high redshift $z \geq 1$ are hosted in bright spheroidal galaxies with a rather evolved stellar population (Dunlop 1999; Zirm et al 1999; Lacy, Bunker and Ridgway 2000; McLure and Dunlop 2000). These observations support our assumption. Also recent photometric and spectroscopic follow-up of a hard X-ray selected sample showed that a large fraction of the $z \gtrsim 1$ AGN, responsible for a major fraction of the HXRb, are hosted in early type optically luminous galaxies (Barger et al 2000).

Observations of radio quiet QSO hosts show that their luminosity at fixed QSO luminosity decrease with increasing

z , (McLure et al 1999; Ridgway et al 1999; Rix et al 1999). The 5 QSOs with $z \geq 1.7$ studied by Rix et al (1999) exhibit a median ratio of the nuclear to the host galaxy luminosity $L_N/L_{host} \simeq 6$ in the V-band, while in the R-band for 9 low redshift ($z \leq 0.24$) QSOs McLure et al (1999) found $L_N/L_{host} \simeq 1.5$. This decrease by a factor 4 is explained by the observed decline of the median Eddington ratio from $L/L_{Edd} \sim 1-2$ to $L/L_{Edd} \simeq 0.1-0.2$ for QSO at high redshift and low redshift respectively (Padovani 1989; Sun and Malkan 1989; Wandel 1999). As a matter of fact the low redshift radio quiet QSO of the sample of McLure et al (1999) exhibit a median $L/L_{Edd} \simeq 0.2$, under the assumption that $M_{bh}/M_{sph} \simeq 3 \times 10^{-3}$.

The observed decrease of the L/L_{Edd} ratio is expected in our scenario. When QSOs shine at high redshift $z \geq 1.5-2$ they have still large gas reservoirs in the hosts and they can reach the self-regulated Eddington accretion. At lower redshift, gas in hosts is scanty and only encounters with other galaxies can supply material for re-activation. However this supply can only occasionally be large enough to reach the self-regulated regime (see also Cavaliere and Vittorini 2000). Note that the decrease of L/L_{Edd} is quantitatively reproduced by the semi-analytic model by Kauffmann and Haehnelt (2000). In this case however it is driven not only by the lower gas fraction left at lower redshift, but also by the adopted redshift dependence of the accretion timescale $t_{acc} \propto (1+z)^{-1.5}$ in their best fit model.

7.2 Early baryon collapse in massive DM haloes

The hierarchical scheme in the Dark Matter component can naturally explain the onset of QSO activity and of star formation in spheroids. In particular the Press-Schechter formalism within the standard variants predicts a large enough number of massive DM halos in order to host QSOs and their parent galaxies (see e.g. Haehnaelt and Rees 1993; Haehnaelt, Natarajan and Rees 1998; Cattaneo, Haehnaelt and Rees 1999; Monaco, Salucci and Danese 2000). However a distinct character of hierarchical DM scheme is that smaller haloes virialize earlier. On the other hand the high SFRs and IR luminosities implied by the far-IR counts exclude that most of the stars have formed in smaller subclumps at very high redshifts, say $z \sim 10$. It is plausible that at high redshift $z \gtrsim 6$ the SFR has been kept very low in the subclumps by 'internal' mechanisms (e.g. SN feedback or even a low activity of the nucleus), which became progressively ineffective when larger and larger masses virialized. Then, as discussed in Sect. 2.2, a significant fraction of the baryons in massive 'virialized' haloes can fragment very rapidly to form stars and QSOs, while the star formation is further delayed in smaller haloes by the effect of stellar feedback. The shining of the QSOs is the final and brief time episode of the complex processes involved in assembling baryons in stars and BH. Most of the relevant observational facts can be framed in a scenario in which the most massive objects complete their activity in a very short time interval $T_{burst} \simeq 0.5$ Gyr and the less massive in ~ 2 Gyr. In a sense the DM hierarchical sequence is corrected by an *Anti-hierarchical Baryonic Collapse* (see also paper II), regulated by the QSO and SN feedback.

Since star formation in massive ellipticals occurs early

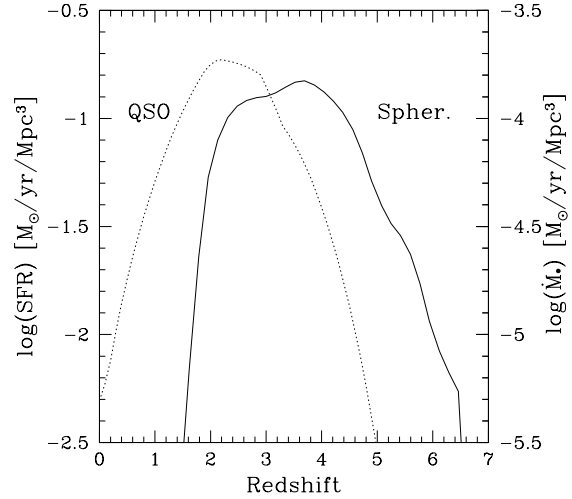


Figure 8. Star formation (solid line and data points, left scale) and mass accretion (dotted line, right scale) rates per unit volume as functions of redshift. The latter has been derived from the data on QSO luminosity function evolution as a function of redshift. The SFR refers to the Case A.

and in relatively short times, the emerging picture is somewhat in between the concept of a 'monolithic' collapse of baryons inside the haloes and the 'classical' hierarchical semi-analytic models, discussed for instance by Kauffmann & Charlot (1998) and Governato et al. (1998). In particular, the connection between ellipticals and quasars has been addressed recently by Kauffmann & Haehnelt (2000). In their 'classical' scenario of the merging process they reproduce the QSO activity decline, but the most massive spheroids form late. As a result they predict a significant active evolution of the host galaxy after the quasar shines. On the contrary in our scheme the host galaxies evolve passively, except for subsequent minor mergers at lower redshift which change the mass in stars by no more than 20% (Trager et al. 2000b; see also Van Dokkum et al. 1999).

It is very likely that the main aspects of the *Anti-hierarchical Baryonic Collapse* can be reproduced by semi-analytical models, by acting on very basic parameters, such as merging and star formation timescales and SN feedback efficiency.

7.3 The star formation in spheroids

The star formation rate per unit volume $\dot{\rho}_*$ in spheroids as a function of redshift derived from our modelling is presented in Fig. 8. The mass accretion rate per unit volume implied by the observed nuclear activity is also presented. It is apparent that in our scheme the star formation rate in QSO hosts is rapidly falling down at $z \lesssim 2$. However the star formation rate in the Universe remains significant because of the star formation in discs and dwarves.

The star formation rate inferred, without dust correction from the UV emission of LBGs galaxies at $z \geq 3$ is a factor ~ 5 lower than our prediction (Steidel et al 1999).

However this is consistent with the evidence of strong extinction of UV emission.

The density of mass cycled through stars in QSO hosts amounts to $\rho_{c\star} \simeq 3.2 \times 10^8 M_{\odot} \text{ Mpc}^{-3}$, which implies (using Salpeter IMF) a present density of long-lived stars in QSO hosts $\rho_{\star} \simeq 2 \times 10^8 M_{\odot} \text{ Mpc}^{-3}$. This mass density can be compared to the mass density in stars in local spheroids $2 \times 10^8 \leq \rho_{\star}^{sph} \leq 5 \times 10^8 M_{\odot} \text{ Mpc}^{-3}$ (Fukugita et al 1999). The metal mass density is roughly given by $\rho_Z \simeq y_Z \rho_{c\star} \simeq 9 \times 10^6 M_{\odot} \text{ Mpc}^{-3}$, y_Z denoting the fraction of metals returned to the interstellar matter by a stellar generation (0.028 with the adopted IMF). In our scenario only about 40% of these metals are still locked into stars, while the rest are spread over the intergalactic medium. The X-ray emitting gas in groups and clusters of galaxies amounts to $\rho_{IGM}(z=0) \simeq 1 \times 10^9 M_{\odot} \text{ Mpc}^{-3}$ (Fukugita et al. 1999). Available observations suggest that this gas has $Z \simeq 1/3 Z_{\odot}$ (Renzini 1999), implying $\rho_Z \text{ IGM}(z=0) \simeq 7 \times 10^6 M_{\odot} \text{ Mpc}^{-3}$, not far from our prediction.

8 SUMMARY

We have presented a unifying scheme for the formation of QSOs, elliptical and S0 galaxies, and for the bulges of spirals. We have shown that the main aspects of the evolution of spheroidal galaxies and QSOs can be well understood if we assume at $t = t_{QSO}$, when the QSOs shine, the bulk of the stars have already been formed in QSO hosts with star formation lasting a time $T_{burst} = t_{QSO} - t_{\star}$ ranging from ~ 0.5 to ~ 2 Gyr when going from more to less massive hosts. This suggest an *Anti-hierarchical Baryonic Collapse*, i.e. that the baryons in large spheroids collapse very rapidly to form stars and QSOs, while the collapse of baryons in smaller spheroids is slowed down. In fact we have shown that the central regions of the massive DM haloes can form stars on very short timescales, while the SNe feedback is strongly slowing down the SFR in small spheroids, extending the star forming phase. The ensuing formation rates scale as $SFR \simeq 100 (M/10^{11} M_{\odot})^{1.3} M_{\odot} \text{ yr}^{-1}$. In our picture when the QSO reaches its maximum, the combined actions of its power and SN feedback are able to practically stop both the SFR and the nuclear accretion through ionization, heating and winds. This influences both the mass in stars M_{sph} and the BH mass M_{BH} and may be the origin of the observed correlation between the two masses. As a result only about 20-40% of the baryons are presently in stars both in massive and small DM galactic haloes. The remaining is in warm or hot gas with $Z \simeq \frac{1}{3} Z_{\odot}$. The outlined scenario can explain:

- (1) the main aspects of the chemical evolution of spheroids (stellar metallicity, luminosity-metallicity relationship, the α enhancement) and the observed elemental abundances in QSOs;
- (2) the 850 source counts;
- (3) the main properties of Lyman Break Galaxies;
- (4) the detection of high redshift, red and old massive ellipticals.

This general view implies the following evolution sequence for QSO hosts:

- (i) the most massive appear, at high redshifts $z \gtrsim 2-6$, as

ultraluminous far-IR galaxies (SCUBA galaxies). This phase lasts for $T_{burst} \sim 0.5 - 1$ Gyr. On the average they are optically faint $I_{AB} \gtrsim 26 - 27$ with colors difficult to predict, in the sense that, depending on uncertain details of dust distribution, both objects with some intrinsic UV emission as LBGs and very red objects (like EROs) can be expected;

- (ii) the hosts of intermediate and low mass have bursts more protracted $T_{burst} \sim 1 - 2$ Gyr and at $z \geq 3$ can appear as LBGs;

- (iii) the QSO phase then follows. The IR emission is attributable both to the starburst and the nuclear activity. This phase lasts for the QSO duty cycle $\Delta t_Q \simeq t_{duty} \simeq 4 \times 10^7 \text{ yr}$. It ends because heating, and ionization of the ISM and the possible onset of galactic winds drastically reduce SFR and nuclear activity;

- (iv) a long epoch of passive evolution follows, with spectra becoming quickly red.

The scheme implies that 850 μm selected galaxies with $S_{850} \geq 1 \text{ mJy}$ are strongly clustered. Also LBGs are expected to be significantly clustered, though to a lower level.

The emerging picture is consistent with hierarchical models for structure formation. However it evidences that, in order to understand key observations of QSOs and elliptical galaxies, the hierarchical assembly of DM haloes must be completed by the history of the baryons inside the haloes themselves. The physical processes related to star formation and feedback suggest that baryons can collapse in stars and QSO more rapidly in more massive haloes. However why the QSOs shine in their hosts when star formation has already progressed, is still an open problem.

ACKNOWLEDGEMENTS

We thank Alessandro Bressan, Cesare Chiosi and Francesca Matteucci for helpful discussions and David Borg for careful reading of the manuscript. We also thank ASI and italian MURST for financial support.

REFERENCES

- Adelberger K.L., Steidel C.C., 2000, astro-ph 0001126
 Andreani P., Franceschini A., Granato G.L., 1999, MNRAS, 306, 161
 Archibald E.N., Dunlop J.S., Hughes D.H., Rawlings S., Eales S.A., Ivison R.J., 2000, astro-ph 0002083
 Arimoto N., Yoshii Y., 1986, A&A, 164, 260
 Balland C., Silk J., Schaeffer R., 1998, ApJ, 497, 541
 Barger A.J., Cowie L.L., Sanders D.B., 1999, ApJ, 518, L5
 Barger A.J., Cowie L.L., Mushotzky R.F., Richards E.A., 2000, ApJ submitted, astro-ph 0007175
 Barger A.J., Cowie L.L., Richards E.A., 2000, AJ, 119, 2092
 Bautz M.W., Malm M.R., Baganoff F.K., Ricker G.R., Canizares C.R., Brandt W.N., Hornschemeier A.E., Garmire G.P., 2000, ApJ in press, astro-ph 0008050
 Benford D.J., Cox P., Omont A., Phillips T.G., Mc Mahon R.G., 1999, ApJ, 518, L65
 Bernardi M., Renzini A., Da Costa L.N., Wegner G., Alonso M.V., Pellegrini P.S., Ritè C., Willmer C.N.A., 1998, ApJ, 508, L143
 Blain A.W., Jameson A., Smail I., Longair M.S., Kneib J.P., Ivison R.J., 1999a, MNRAS, 309, 715
 Blain A.W., Kneib J.P., Ivison R.J., Smail I., 1999b, ApJ, 512, L87

- Blain A.W., Smail I., Ivison R., Kneib J., 1999c, in Bunker A.J., van Breugel W.J.M., eds., ASP Conf. Ser. The Hy-redshift universe: galaxy formation and evolution at high redshift, Vol. 193, p. 425
- Bower R.G., Lucey J.R., Ellis R.S., 1992, MNRAS, 254, 601
- Boyle B.J., Griffiths R.E., Shanks T., Stewart G.C., Georgantopoulos I., 1993, MNRAS, 260, 49
- Borys C., Chapman S. C., Halpern M., Scott D., 2000, astro-ph/0009067
- Bressan A., Chiosi C., Fagotto F., 1994, ApJS, 94, 63
- Bruzual A.G., 1983, ApJ, 273, 105
- Bruzual A.G., Charlot S., 1993, ApJ, 405, 538
- Cattaneo A., Haehnelt M., Rees M.J., 1999, MNRAS, 308, 77
- Cavaliere A., Vittorini V., 2000, ApJ submitted, astro-ph 0006194
- Chapman S.C., Scott D., Steidel C.C., Borys C., Halpern M., Morris S.L., Adelberger K.L., Dickinson M., Giavalisco M., Pettini M., 1999, MNRAS, submitted (astro-ph/9909092)
- Chapman S.C., Scott D., Borys C., Fahlman G. G., 2000, astro-ph/0009067
- Cimatti A., Andreani P., Rottgering H., Tilanus R., 1998, Nature, 392, 895
- Comastri A., Setti G., Zamorani G., Hasinger G., 1995, A&A, 296, 1
- Condon J.J., Yin Q.F., 1990, ApJ, 357, 97
- Connolly A.J., Szalay A.S., Dickinson M., Subbarao M.U., Brunner R.J., 1997, ApJ, 486, L11
- Dekel A., Silk J., 1986, ApJ, 303, 1986
- Dey A., Graham J.R., Ivison R.J., Smail I., Wright G.S., Liu M.C., 1999, ApJ, 519, 610
- Draine B.T., Lee H.M., 1984, ApJ, 285, 89
- Dunlop J.S., 1999, in Bunker A.J., van Breugel W.J.M., eds., ASP Conf. Ser. The Hy-redshift universe: galaxy formation and evolution at high redshift, Vol. 193, p. 133
- Eales S., Lilly S., Webb T., Dunne L., Gear W., Clements D., Yun M., 2000 astro-ph/0009154
- Efstathiou A., Rowan-Robinson M., 1995, MNRAS, 273, 649
- Efstathiou A. et al., 2000, MNRAS, submitted
- Ellis R.S., Smail I., Dressler A., Couch W.J., Oemler A. JR., Butcher H., Sharples R.M., 1997, ApJ, 483, 582
- Fabian A.C., 1999, MNRAS, 308, L39
- Fabian A.C., Smail I., Iwasawa K., Allen S.W., Blain A.W., Crawford C.S., Etori S., Ivison R.J., Johnstone R.M., Kneib J.-P., Wilman R.J., 2000, MNRAS 315, L8
- Ferrarese, L., Merritt, D., 2000, ApJ 539, L9 0006053
- Fisher D., Franx M., Illingworth G., 1995, ApJ, 448, 119
- Fixsen D.J., Dwek E., Mather J.C., Bennett C.L., Shafer R.A., 1998, ApJ, 508, 123
- Fontana, A., Menci, N., D'Odorico, S., Giallongo, E., Poli, F., Cristiani, S., Moorwood, A., Saracco, P., 1999, MNRAS, 310, L27
- Franceschini A., Silva L., Fasano G., Granato G.L., Bressan A., Arnouts S., Danese L., 1998, ApJ, 506, 600
- Frayser D.T., Smail I., Ivison R.J., Scoville N.Z., 2000, astro-ph 0005239
- Fukugita M., Hogan C.J., Peebles P.J.E., 1998, ApJ, 503, 518
- Gebhardt K., Bender R., Bower G., Dressler A., Faber S.M., Filippenko A.V., Green R., Grillmair C., Ho L.C., Kormendy J., Lauer T.R., Magorrian J., Pinkey J., Richstone D., Tremaine S., 2000, ApJ 539, L13
- Genzel R., Lutz D., Sturm E., Egami E., Kunze D., Moorwood A.F.M., Rigopoulou D., Spoon H.W.W., Sternberg A., Tacconi-Garman L.E., Tacconi L., Thatte N., 1998, ApJ, 498, 579
- Giacconi R., Rosati P., Tozzi P., Nonino M., Hasinger G., Norman C., Bergeron J., Borgani S., Gilli R., Gilmozzi R., Zheng W., 2000, astro-ph 0007240
- Governato F., Baugh C.M., Frenk C.S., Cole S., Lacey C.G., Quinn T., Stadel J., 1998, Nature, 392, 359
- Granato G.L., Danese L., 1994, MNRAS, 268, 235
- Granato G.L., Danese L., Franceschini A., 1997, ApJ, 486, 147
- Granato, G.L., Lacey, C.G., Silva, L., Bressan, A. Baugh, C.M., Cole, S., Frenk, C.S., 2000, ApJ, October 2000 (astro-ph/0001308)
- Grazian A., Cristiani S., D'Odorico V., Omizzolo A., Pizzella A., 2000, AJ, 119, 2540
- Guiderdoni B., Hivon E., Bouchet F.R., Maffei B., 1998, MNRAS 295, 877
- Gunn K.F., Shanks T., 1999, MNRAS submitted, astro-ph 9909089
- Haehnelt M.G., Rees M.J., 1993, MNRAS, 263 168
- Haehnelt M.G., Natarajan P., Rees M.J., 1998, MNRAS 300, 817
- Hamann F., Ferland G., 1993, ApJ, 418, 11
- Hamann F., Ferland G., 1999, ARA&A, 37, 487
- Hornschemeier A.E., Brandt W.N., Garmire G.P., Schneider D.P., Broos P.S., Townsley L.K., Bautz M.W., Burrows D.N., Chartas G., Feigelson E.D., Griffiths R., Lumb D., Nousek J.A., Sargent W.L.W., 2000, ApJ, 541, 49
- Hu E.M., Ridgway S.E., 1994, AJ, 107, 1303
- Hughes et al., 1998, Nature, 394, 241
- Im M., Griffiths R., Ratnatunga K., Sarajedini V., 1996, ApJ, 461, 79
- Ivison R.J., Smail I., Le Borgne J.F., Blain A.W., Kneib J.P., Bezecourt J., Kerr T.H., Davies J.K., 1998, MNRAS, 298, 583
- Ivison R.J., Smail I., Barger A.J., Kneib J.P., Blain A.W., Owen F.N., Kerr T.H., Cowie L.L., 2000, MNRAS, 315, 209
- Jablonska P., Martin P., Arimoto N., 1996, AJ, 112, 1415
- Kauffmann G., Guiderdoni B., White S.D.M., 1994, MNRAS, 267, 981
- Kauffmann G., Charlot S., White S.D.M., 1996, MNRAS, 283, 117
- Kauffmann G., Charlot S., 1998, MNRAS, 297, L23
- Kauffmann G., Haehnelt M., 2000, MNRAS, 311, 576
- Kawara K., Sato Y., Matsuhara H., Taniguchi Y., Okuda H., Sofue Y., Matsumoto T., Wakamatsu K., Karoji H., Okamura S., Chambers K.C., Cowie L.L., Joseph R.D., Sanders D.B., 1998, A&A, 336, L9
- Kennefick J.D., Djorgovski S.G., Meylan G., 1996, AJ, 111, 1816
- Kobayashi C., Tsujimoto T., Nomoto K., 2000, ApJ, 539, 26
- Kobayashi C., Arimoto N., 1999, ApJ, 527, 573
- Kodama T., Arimoto N., Barger A.J., Aragon-Salamanca A., 1998, A&A, 334, 99
- Lacy M., Bunker A.J., Ridgway S.E., 2000, AJ, 120, 68
- Larson R.B., 1974, MNRAS, 169, 229
- Madau P., Ferguson H.C., Dickinson M., Giavalisco M., Steidel C.C., Fruchter A., 1996, MNRAS, 283, 1388
- Magorrian J., Tremaine S., Richstone D., Bender R., Bower G., Dressler A., Faber S.M., Gebhardt K., Green R., Grillmair C., Kormendy J., Lauer T., 1998, AJ, 115, 2285
- Martini P., Wienberg D.H., 2000, ApJ submitted, astro-ph0002384
- Mathews W.G., Baker J.C., 1971, ApJ, 170, 241
- Matteucci F., 1994, A&A, 288, 57
- McLure R.J., Kukula M.J., Dunlop J.S., Baum S.A., O'Dea C.P., Huges D.H., 1999, MNRAS, 308, 377
- McLure R.J., Dunlop J.S., 2000, MNRAS, 317, 249
- Miyaji T., Hasinger G., Schmidt M., 2000, A&A, 353, 25
- Monaco P., Salucci P., Danese L., 2000, MNRAS, 311, 279 (paper II)
- Mushotzky R.F., Cowie L.L., Barger A.J., Arnaud K.A., 2000, Nat, 404, 459
- Navarro J.F., Frenk C.S., White S.D.M., 1997, ApJ 490, 493
- Omont A., Petitjean P., Guilloteau S., McMahan R.G., Solomon P.M., Pecontal E., 1996, Nature, 382, 4280
- Padovani P., 1989, A&A, 209, 27
- Peacock J.A., Rowan-Robinson M., Blain A.W., Dunlop J.S., Ef-

- stathiou A., Hughes D.H., Jenness T., Ivison R.J., Lawrence A., Longair M.S., Mann R.G., Oliver S.J., Serjeant S., 1999, MNRAS, in press (astro-ph/9912231)
- Pei Y.C., 1995, ApJ, 438, 623
- Puget J.L., Lagache G., Clements D.L., Reach W.T., Aussel H., Bouchet F.R., Cesarsky C., Dsert F.X., Dole H., Elbaz D., Franceschini A., Guiderdoni B., Moorwood A.F.M., 1999, A&A, 345, 29
- Renzini A., 1997, ApJ, 488, 35
- Renzini A., 1999, in Carollo C.M., Ferguson H.C., Wyse R.F.G., eds., The formation of galactic bulges. Cambridge University Press, p. 9
- Renzini A., 2000, in Large Scale Structure in the X-ray Universe, Plionis M., Georgantopoulos I., eds, Atalasciences, Paris, p. 103
- Richstone D., Ajhar E.A., Bender R., Bower G., Dressler A., Faber S.M., Filippenko A.V., Gebhardt K., Green R., Ho L.C., Kormendy J., Lauer T., Magorrian J., Tremaine S., 1998, Nature, 395, 14
- Ridgway S., Heckman T., Calzetti D., Lehnert M., 1999, astro-ph/9911049
- Rix H-W., Falco E., Impey C., Kochanek C., Lehar J., McLeod B., Munoz J., peng C., 1999, astro-ph/9910190
- Salucci P., Szuszkiewicz E., Monaco P., Danese L., 1999, MNRAS, 307, 637 (paper I)
- Sanders D.B., Soifer B.T., Elias J.H., Madore B.F., Matthews K., Neugebauer G., Scoville N.Z., 1988, ApJ, 325, 74
- Schade D., Lilly S.J., Crampton D., Ellis R.S., Le Fevre O., Hammer F., Brinchmann J., Abraham R., Colless M., Glazebrook K., Tresse L., Broadhurst T., 1999, ApJ, 525, 31
- Scott D., Lagache G., Borys C., Chapman S.C., Halpern M., Sajina A., Ciliegi P., Clements D.L., Dole H., Oliver S., Puget J.L., Reach W.T., Rowan-Robinson M., 2000, A&A, 357, L5
- Severgnini P., Maiolino R., Salvati M., Axon D., Cimatti A., Fiore F., Gilli R., La Franca F., Marconi A., Matt G., Risaliti G., Vignali C., 2000, A&A, 360, 457
- Sutherland R., Dopita M.A., 1993, ApJS, 88, 253
- Silk J., Rees M.J., 1998, A&A, 331, L1
- Silva L., Granato G.L., Bressan A., Danese L., 1998, ApJ, 509, 103
- Silva L., 1999, PhD thesis, SISSA, Trieste
- Smail I., Ivison R.J., Kneib J.P., Cowie L.L., Blain A.W., Barger A.J., Owen F.N., Morrison G.E., 1999, MNRAS, 308, 1061
- Smail I., Ivison R.J., Owen F.N., Blain A.W., Kneib J.P., 2000, ApJ, 528, 612
- Steidel C.C., Pettini M., Hamilton D., 1995, AJ, 110, 2519
- Steidel C.C., Giavalisco M., Dickinson M., Adelberger K.L., 1996, AJ, 112, 352
- Steidel C.C., Adelberger K.L., Giavalisco M., Dickinson M., Pettini M., 1999, ApJ, 519, 1
- Sun W.H., Malkan M.A., 1989, ApJ 346, 68
- Tan J.C., Silk J., Balland C., 1999, ApJ, 522, 579
- Thomas D., Greggio L., Bender R., 1999, MNRAS, 302, 537
- Trager S.C., Faber S.M., Worthey G., Gonzalez J.J., 2000a , AJ 119, 1645
- Trager S.C., Faber S.M., Worthey G., Gonzalez J.J., 2000b , AJ, 120, 165
- van der Marel R.P., 1999, AJ, 117, 744
- van Dokkum P.G., Franx, M., Fabricant, D., Kelson, D.D., Illingworth, G.D., 1999, ApJ, 520, L95
- Wandel A., 1999, in Quasar Broad Line Regions, Gaskell C.M., Brandt W.N., Dietrich M., Dultzin-Hacyan D., and M. Eracleous eds., ASP. Conf. Ser. vol. 175, p.213
- White S.D.M., Frenk C.S., 1991, ApJ, 379, 52
- Yun M.S., Carilli C.L., Kawabe R., Tutui Y., Kohno K., Ohta K., 200, ApJ, 528, 171
- Zirm A., Dey A., Dickinson M., McCarthy P.J., Eisenhardt P., Djorgovski S.G., Spinrad H., Stanford S.A., van Breugel W., 1999, in Bunker A.J., van Breugel W.J.M., eds., ASP Conf. Ser. The Hy-redshift universe: galaxy formation and evolution at high redshift, Vol. 193, p. 114

This paper has been produced using the Royal Astronomical Society/Blackwell Science L^AT_EX style file.